ORIGINAL ARTICLE

Multi-GNSS real-time precise clock estimation considering the correction of inter-satellite code biases

Liang Chen[1,2,3] · Min Li[3] · Ying Zhao[4] · Zhigang Hu[3] · Fu Zheng[1,5] · Chuang Shi[1,5]

Abstract

For reasons mostly related to chip shape distortions, global navigation satellite system (GNSS) observations are corrupted by receiver-dependent biases. These are often stable in the long term, though numerically different depending on the signal frequency, satellite system and receiver manufacturer. Based on the mixed-differenced model combining undifferenced pseudorange with epoch-differenced carrier phase observations, we present a multi-GNSS real-time precise clock estimation model considering correction of inter-satellite code biases (ISCBs). Pre-estimated receiver-dependent ISCB corrections are introduced to correct the inter-receiver, inter-satellite and inter-system biases largely. Then the number of estimated parameters is reduced to a manageable level for real-time estimation. Comparisons with post-processed data show that compared to undifferenced, epoch-differenced and non-bias-corrected mixed-differenced models, the proposed bias-corrected model can greatly reduce the precise clock offset systematic biases, especially for GLONASS and BeiDou. The test results show the root mean square data reductions are improved by up to 96% for GLONASS, 78% for BeiDou and 40% for GPS and Galileo.

Abbreviations

AC	Analysis center
cIFB	Code IFB
ED	Epoch-differenced
GNSS	Global navigation satellite system
IFB	Inter-frequency bias
IGS	International GNSS service
ISCB	Inter-satellite code bias
MD	Mixed-differenced
OMC	Observed minus calculated
TGD	Timing group delay
UD	Undifferenced

✉ Zhigang Hu
zhigang.hu@whu.edu.cn

✉ Fu Zheng
fzheng@buaa.edu.cn

1 School of Electronic and Information Engineering, Beihang University, 37 Xueyuan Road, Beijing 100191, China

2 Shanghai Key Laboratory of Space Navigation and Positioning Techniques, Shanghai 200030, China

3 GNSS Research Center, Wuhan University, 129 Luoyu Road, Wuhan 430079, China

4 National Quality Inspection and Testing Center for Surveying and Mapping Products, 28 Lianhuachi West Road, Beijing 100830, China

5 Research Institute for Frontier Science, Beihang University, 37 Xueyuan Road, Beijing 100191, China

Introduction

To provide precise positioning services based on state space representation (SSR), such as precise point positioning (PPP) and PPP-real-time kinematic (PPP-RTK), precise satellite orbits and clocks should be estimated and broadcast to users in real time (Wübbena et al. 2005; Ge et al. 2012). At present, the International GNSS Service (IGS) is providing ultra-rapid orbit products, including 24-h observation orbits and 24-h forecast orbits (http://www.igs.org).

IGS initiated the Real-Time Pilot Project through a call-for-participation[1] in June 2007. Currently, the IGS provides GPS and GLONASS real-time precise clock products with an accuracy of 0.3–0.8 ns (Hadas and Bosy 2015). The utilization of frequency-division multiple access (FDMA) communication causes the GLONASS pseudorange and carrier phase observations to suffer from variable levels of inter-frequency bias (IFB) (Song et al. 2014; Chen et al. 2018a).

Moreover, different IGS ACs eliminate the GLONASS code IFBs (cIFBs) impact in different ways, leading to significant biases in the satellite- and AC-specific offsets in the GLONASS precise clocks. Furthermore, the GLONASS cIFBs also lead to day-boundary jumps between consecutive days in the GLONASS precise clock for the same AC (Song et al. 2014).

A series of achievements have been attained by optimizing and improving the traditional real-time clock estimation model. Based on the precise clock products with 5-min sampling intervals obtained in the precise orbit determination process, the Center for Orbit Determination in Europe (CODE) has achieved real-time clock broadcasting by fixing the station coordinates, Earth rotation parameters and tropospheric parameters (Bock et al. 2009). A combined dual-thread algorithm, consisting of an undifferenced engine and an epoch-differenced engine, enables real-time precise clock estimation and can achieve a root mean square (RMS) of about 0.2 ns (Zhang et al. 2011). By using undifferenced pseudorange and epoch-differenced carrier phase together, Ge et al. (2012) introduced a computationally efficient mixed-differenced model for real-time absolute precise clock estimation. Zhang et al. (2016) designed a joint GPS/BeiDou real-time clock estimation model by introducing an inter-satellite single-differenced process based on the mixed-differenced model. The clock accuracy is approximately 0.6 ns RMS and 0.1 ns standard deviation (STD) and estimation efficiency per epoch is less than 0.4 s based on a 100-station network (Zhang et al. 2016). A modified mixed-differenced model proposed by Chen et al. (2018c) achieved multi-GNSS real-time clocks STDs of approximately 0.1–0.4 ns and RMSs of 0.4–2.3 ns, where GLONASS and BeiDou clocks have a large systematic bias.

The satellite-dependent code bias has been included in the satellite clock products provided by the IGS based on ionospheric-free combined observations (Montenbruck et al. 2017) and is generally considered ignorable in ionospheric-free combined PPP using IGS precise products (Schaer et al. 1998). However, in precise clock solutions based on four independent global networks composed of Javad-only, Leica-only, Trimble-only and Septentrio-only receivers, Hauschild et al. (2019) found that there were different clock offset biases. These biases exhibit long-term consistency in inter-manufacturer network solutions and the differences can reach several nanoseconds, which will directly cause the absolute accuracy of a precise clock to degrade.

On the receiver side, pseudorange signals of GNSS satellites are subject to individual chip shape distortions. Similar to the effect of multipath signal reflections, these distortions lead to different shifts of the correlator's tracking point for each PRN, which then results in a different inter-satellite code biases (ISCBs) for each satellite (Hauschild et al. 2019; He et al. 2020). Pseudorange observations tracked by receivers with different correlator- and/or front-end design exhibit different ISCBs. Hauschild and Montenbruck (2016) verified the existence of inter-receiver code biases based on different receiver types for zero baselines and found that the inter-receiver differences of the GLONASS cIFBs and code-division multiple access (CDMA) ISCBs could reach 1–2 m. Notably, the receiver-dependent ISCB of each manufacturer remains stable over a long time; the STDs for GPS and Galileo are at the centimeter level. For GLONASS is at the decimeter level (Shi et al. 2013; Chen et al. 2018a).

With the construction of BeiDou and Galileo, more navigation satellites have been introduced into the combined estimation process. Especially because of the FDMA characteristics of GLONASS signals, for multi-GNSS high-precision fusion applications, it is necessary to study how to eliminate the systematic biases in clock offset estimation and efficiently obtain real-time absolute precise clock products. We present a multi-GNSS real-time precise clock estimation approach considering ISCB correction. On the basis of using undifferenced pseudorange and epoch-differenced carrier phase observations to eliminate ambiguity parameters, an ISCB correction process is additionally introduced to eliminate these systematic biases. Then, we analyze the performance of real-time precise clock estimation model considering ISCB correction.

Methodology

For the convenience of methodological description, we first introduce the observations considering ISCBs and then analyze the features of current undifferenced and epoch-differenced models. The principal acronyms used are summarized at the end.

Observations considering ISCBs

GNSS dual-frequency ionospheric-free (IF) combined observations considering satellite- and receiver-dependent ISCBs can be expressed as follows:

$$
\begin{cases}
P^{s,G_i}_{r,\mathrm{IF}} = \rho^{s,G_i}_r + \mathrm{d}t_r + b^{s,G_i}_{r,P,\mathrm{ISCB}} - \left(\mathrm{d}t0^{s,G_i} + \mathrm{d}t^{s,G_i}\right) - B^{s,G_i}_P + M^{s,G_i}_r \cdot \mathrm{zwd} + \varepsilon^{s,G_i}_P \\
\Phi^{s,G_i}_{r,\mathrm{IF}} = \rho^{s,G_i}_r + \mathrm{d}t_r + b^{s,G_i}_{r,\Phi} - \left(\mathrm{d}t0^{s,G_i} + \mathrm{d}t^{s,G_i}\right) - B^{s,G_i}_\Phi + N^{s,G_i}_r + M^{s,G_i}_r \cdot \mathrm{zwd} + \varepsilon^{G_i}_\Phi \\
P^{s,R_j}_{r,\mathrm{IF}} = \rho^{s,R_j}_r + \mathrm{d}t_r + b^{s,R_j}_{r,P,\mathrm{ISCB}} - \left(\mathrm{d}t0^{s,R_j} + \mathrm{d}t^{s,R_j}\right) - B^{s,R_j}_P + M^{s,R_j}_r \cdot \mathrm{zwd} + \varepsilon^{s,R_j}_P \\
\Phi^{s,R_j}_{r,\mathrm{IF}} = \rho^{s,R_j}_r + \mathrm{d}t_r + b^{s,R_j}_{r,\Phi} - \left(\mathrm{d}t0^{s,R_j} + \mathrm{d}t^{s,R_j}\right) - B^{s,R_j}_\Phi + N^{s,R_j}_r + M^{R_j}_r \cdot \mathrm{zwd} + \varepsilon^{R_j}_\Phi \\
P^{s,C_k}_{r,\mathrm{IF}} = \rho^{s,C_k}_r + \mathrm{d}t_r + b^{s,C_k}_{r,P,\mathrm{ISCB}} - \left(\mathrm{d}t0^{s,C_k} + \mathrm{d}t^{s,C_k}\right) - B^{s,C_k}_P + M^{s,C_k}_r \cdot \mathrm{zwd} + \varepsilon^{s,C_k}_P \\
\Phi^{s,C_k}_{r,\mathrm{IF}} = \rho^{s,C_k}_r + \mathrm{d}t_r + b^{s,C_k}_{r,\Phi} - \left(\mathrm{d}t0^{s,C_k} + \mathrm{d}t^{s,C_k}\right) - B^{s,C_k}_\Phi + N^{s,C_k}_r + M^{C_k}_r \cdot \mathrm{zwd} + \varepsilon^{C_k}_\Phi \\
P^{s,E_m}_{r,\mathrm{IF}} = \rho^{s,E_m}_r + \mathrm{d}t_r + b^{s,E_m}_{r,P,\mathrm{ISCB}} - \left(\mathrm{d}t0^{s,E_m} + \mathrm{d}t^{s,E_m}\right) - B^{s,E_m}_P + M^{s,E_m}_r \cdot \mathrm{zwd} + \varepsilon^{s,E_m}_P \\
\Phi^{s,E_m}_{r,\mathrm{IF}} = \rho^{s,E_m}_r + \mathrm{d}t_r + b^{s,E_m}_{r,\Phi} - \left(\mathrm{d}t0^{s,E_m} + \mathrm{d}t^{s,E_m}\right) - B^{s,E_m}_\Phi + N^{s,E_m}_r + M^{E_m}_r \cdot \mathrm{zwd} + \varepsilon^{E_m}_\Phi
\end{cases}
\tag{1}
$$

where P and Φ represent the ionospheric-free pseudorange and carrier phase functions corrected for dry tropospheric delay using a model. The superscript s identifies the satellite and the subscript r identifies the receiver. $G_i = i$th GPS, $R_j = j$th GLONASS, $C_k = k$th BeiDou, $E_m = m$th Galileo in one epoch. Further, ρ is the traveled geometric distance between satellite to receiver for the instances of transmission and reception of the signal, $\mathrm{d}t_r$ and $\mathrm{d}t^s$ represent the receiver and satellite clock errors. $\mathrm{d}t0^s$ represents the clock offset biases. N is the ambiguity (in meters). The zenith wet delay zwd is estimated from the observations using the wet mapping function M. ε is the observation noise of the respective ionospheric-free function. b and B represent the ionospheric-free receiver- and satellite-dependent signal delay biases, respectively.

The carrier biases, $b^s_{r,\Phi}$ and B^s_Φ, are generally called uncalibrated phase delays (UPDs) (Ge et al. 2008), which usually are involved in ambiguity parameters. The pseudorange biases $b^s_{r,P,\mathrm{ISCB}}$ are called receiver-dependent ISCB. As analyzed above, the individual chip shape distortions in ranging signals lead to different shifts in the correlator's tracking point for each PRN and then introduce different ISCBs into the observations (Hauschild et al. 2019). So we add the superscript s to express that ISCBs b is related to satellites, and superscript G_i, R_j, C_k, E_m to distinguish those different satellites.

Hauschild et al. (2019) found there were different clock offset biases in precise clock solutions based on different independent global networks, which can reach several nanoseconds. The clock offset biases $\mathrm{d}t0^s$ can be regarded as clock offset biases relative to datum clock time. In positioning solution based on precise clock products, the coefficients of satellite-dependent $\mathrm{d}t0^s$ and receiver-dependent inter-satellite code bias $b^s_{r,P,\mathrm{ISCB}}$ in (1) are the same, which makes it difficult to separate the two parameters if no extra constraint. So we absorb $\mathrm{d}t0^s$ into $b^s_{r,P,\mathrm{ISCB}}$ in (1). However, $\mathrm{d}t0^s$ is ignored in precise clock estimation as a part of the estimated clock parameter.

From (1), we can find the parameters of B^s_P and $\mathrm{d}t0^s$ are related to satellite clock $\mathrm{d}t^s$. B^s_P, satellite-dependent code bias, is relatively stable (Dach et al. 2006), which has been actually included in satellite clock products provided by IGS based on ionospheric-free combined observations (Schaer et al. 1998). In addition, broadcast ephemeris also provides the timing group delay (TGD) correction parameters, which are another representations of the satellite-dependent code bias. Similar to the IGS processing strategy, the final estimated clock parameters actually include ionospheric-free satellite-dependent code biases, i.e., $\mathrm{d}\tilde{t}^s = \mathrm{d}t^s + B^s_P$.

Undifferenced model

Based on real-time data streams, real-time precise GNSS clock offsets can be obtained by fixing the real-time satellite orbits, the earth rotation parameters and the station coordinates generated during processing for real-time precise orbit determination.

Current undifferenced model treats the receiver-dependent code biases as a common bias of equal size for CDMA signals, i.e., all GPS observations just include a common bias $b^{s,G}_{r,P,\mathrm{ISCB}}$, same for BeiDou and Galileo. However, for FDMA signals GLONASS observations include different biases $b^{s,R_j}_{r,P,\mathrm{ISCB}}$. Considering that the pseudorange observations mainly provide the initial information in the normal equations, the receiver clock error and the receiver-dependent ISCBs of GPS signal are combined as $\mathrm{d}\tilde{t}_r = \mathrm{d}t_r + b^{s,G}_{r,P,\mathrm{ISCB}}$. $\mathrm{d}t0^s$ is lumped into precise clock offset as a part of estimated clock parameter. Considering known fixed station coordinates, one can simplify the linearized equations for precise real-time clock offset estimation as follows:

$$
\begin{cases}
v^{s,G_i}_P = \mathrm{d}\tilde{t}_r - \mathrm{d}\tilde{t}^{s,G_i} + M^{s,G_i}_r \cdot \mathrm{zwd} - l^{s,G_i}_P \\
v^{s,G_i}_\Phi = \mathrm{d}\tilde{t}_r - \mathrm{d}\tilde{t}^{s,G_i} + \tilde{N}^{s,G_i}_r + M^{s,G_i}_r \cdot \mathrm{zwd} - l^{s,G_i}_\Phi \\
v^{s,R_j}_P = \mathrm{d}\tilde{t}_r - \mathrm{d}\tilde{t}^{s,R_j} + \mathrm{IFB}^{R_j-G} + M^{s,R_j}_r \cdot \mathrm{zwd} - l^{s,R_j}_P \\
v^{s,R_j}_\Phi = \mathrm{d}\tilde{t}_r - \mathrm{d}\tilde{t}^{s,R_j} + \mathrm{IFB}^{R_j-G} + \tilde{N}^{s,R_j}_r + M^{s,R_j} \cdot \mathrm{zwd} - l^{s,R_j}_\Phi \\
v^{s,C_k}_P = \mathrm{d}\tilde{t}_r - \mathrm{d}\tilde{t}^{s,C_k} + \mathrm{ISB}^{C-G} + M^{s,C_k}_r \cdot \mathrm{zwd} - l^{s,C_k}_P \\
v^{s,C_k}_\Phi = \mathrm{d}\tilde{t}_r - \mathrm{d}\tilde{t}^{s,C_k} + \mathrm{ISB}^{C-G} + \tilde{N}^{s,C_k}_r + M^{s,C_k}_r \cdot \mathrm{zwd} - l^{s,C_k}_\Phi \\
v^{s,E_m}_P = \mathrm{d}\tilde{t}_r - \mathrm{d}\tilde{t}^{s,E_m} + \mathrm{ISB}^{E-G} + M^{s,E_m}_r \cdot \mathrm{zwd} - l^{s,E_m}_P \\
v^{s,E_m}_\Phi = \mathrm{d}\tilde{t}_r - \mathrm{d}\tilde{t}^{s,E_m} + \mathrm{ISB}^{E-G} + \tilde{N}^{s,E_m}_r + M^{s,E_m}_r \cdot \mathrm{zwd} - l^{s,E_m}_\Phi
\end{cases}
\tag{2}
$$

Table 1 Estimated parameters in the undifferenced model

Parameters	Receiver clock offset	Satellite click offset	GLONASS IFB	ISB	Tropospheric	Ambiguity
Number	60	110	1440	120	60	2400
Total	4190					

where v denotes the residuals, $\text{IFB}^{R_j-G} = b^{s,R_j}_{r,P,\text{ISCB}} - b^{s,G}_{r,P,\text{ISCB}}$, $\text{ISB}^{C-G} = b^{s,C}_{r,P,\text{ISCB}} - b^{s,G}_{r,P,\text{ISCB}}$ $\text{ISB}^{E-G} = b^{s,E}_{r,P,\text{ISCB}} - b^{s,G}_{r,P,\text{ISCB}}$, $\tilde{N}^s_r = N^s_r - b^s_{r,P,\text{ISCB}} + B^s_P + b^s_{r,\Phi} - B_\Phi$, and l is the observed minus calculated (OMC) difference, where the observed part is the observations of pseudorange and carrier phase and the calculated part is the geometric distance between satellite to receiver calculated by the precise orbit position at signal transmission and station coordinates at signal reception.

Suppose that there are n_T tracking stations and that the total number of satellites in the multi-GNSS network is $n_S = n_G + n_R + n_C + n_E$. Then, the actual parameters to be estimated in the undifferenced model are

$$
\mathbf{X} = \begin{bmatrix} \mathbf{dt_r}_{n_S \times 1} \\ \mathbf{dt^s}_{n_T \times 1} \\ \mathbf{zwd}_{n_T \times 1} \\ \mathbf{ISB}_{2n_T \times 1} \\ \mathbf{IFB}_{n_T \cdot n_R \times 1} \\ \mathbf{N}_{n_T \cdot n_S \times 1} \end{bmatrix} \tag{3}
$$

$\mathbf{dt_r}_{n_S \times 1}$ is a vector with n_s rows and 1 column and following expression is similar. Suppose that 60 stations are tracking approximately 110 GPS, GLONASS, BeiDou and Galileo satellites and those approximately 40 satellites can be observed per station in each epoch. The corresponding parameters for one epoch in the undifferenced real-time clock offset model are shown in Table 1. The total number of estimated parameters per epoch is 4190, which greatly limits the real-time estimation efficiency and prevents the ability to update at 5-s intervals as recommended by the IGS (Zhang et al. 2011; Ge et al. 2012).

As seen from Table 1, there are 2400 ambiguity parameters and 1440 GLONASS IFB parameters in the undifferenced model. The IFB parameters are usually replaced with intersystem bias (ISB) parameters relative to GPS in actual data processing to improve the solution efficiency, which introduces systematic biases into the GLONASS precise clock offset and consequently leads to initial clock biases (Song et al. 2014). Even though these initial clock biases can be absorbed into the ambiguity parameters and do not affect the positioning accuracy after convergence, they will affect the pseudorange observation accuracy, which will degrade the convergence of PPP.

Epoch-differenced Model

The signal delays of receiver- and satellite-dependent pseudorange and carrier phase observations remain relatively stable (Dach et al. 2006; Hauschild and Montenbruck 2016). If there are no cycle slips, then the ambiguity parameters in (2) can be eliminated by taking a single difference between consecutive epochs as follows (Ge et al. 2012; Chen et al. 2018b):

$$
v^s_{\Delta\Phi}(t) = \Delta dt_{r(t)} - \Delta dt^{s(t)} + M^s_r \cdot \Delta \text{zwd}(t) - l^s_{\Delta\Phi}(t) \tag{4}
$$

where Δ represents the single difference between consecutive epochs and t represents the epoch. Therefore, the parameters to be solved in this model include only the changes in the receiver clock, satellite clock and tropospheric parameters. Thus, an external initial satellite clock product needs to be introduced. If we use the initial clock products and sum the clock changes from the initial epoch to the tth epoch, then the clock offsets in the tth epoch can be recovered as follows:

$$
\begin{aligned}
dt_{r(t)} &= dt_{r(0)} + \Delta dt_{r(t)} + \sum_{ii=1}^{t-1} \Delta dt_{r(ii)} \\
dt^{s(t)} &= dt^{s(0)} + \Delta dt^{s(t)} + \sum_{ii=1}^{t-1} \Delta dt^{s(ii)}
\end{aligned} \tag{5}
$$

where $dt_{r(0)}$ and $dt^{s(0)}$ are the initial receiver and satellite clock offset and ii is the iith epoch from 1 to t. The epoch-differenced carrier phase observations can eliminate only continuous ambiguity parameters. In the case of a data interruption, the initial satellite clock and receiver clock will need to be reintroduced. The initial satellite clock offset can be obtained from the broadcast ephemeris or an ultra-rapid clock offset. Therefore, the epoch-differenced model cannot provide continuous and stable real-time absolute clock offsets (Chen et al. 2018b).

Mixed-differenced model with ISCB correction

Taking advantage of the absolute clock provided by the undifferenced model and eliminating the continuous ambiguities of the epoch-differenced model, Ge et al. (2012)

designed a mixed-differenced model for real-time clock estimation.

Considering the existence of unequal receiver-dependent ISCBs, we substitute the clock offsets in (5) into the linearized pseudorange equations in (2) to obtain the following tth epoch mixed-differenced model observation equations considering ISCB:

$$\begin{cases} v_P^{s,G_i}(t) = \mathrm{d}t_{r(0)} - \mathrm{d}\tilde{t}^{s(0),G_i} + b_{r,P,\mathrm{ISCB}}^{s,G_i}(t) - \tilde{l}_P^{s,G_i}(t) \\ v_P^{s,R_j}(t) = \mathrm{d}t_{r(0)} - \mathrm{d}\tilde{t}^{s(0),R_j} + b_{r,P,\mathrm{ISCB}}^{s,R_j}(t) - \tilde{l}_P^{s,R_j}(t) \\ v_P^{s,C_k}(t) = \mathrm{d}t_{r(0)} - \mathrm{d}\tilde{t}^{s(0),C_k} + b_{r,P,\mathrm{ISCB}}^{s,C_k}(t) - \tilde{l}_P^{s,C_k}(t) \\ v_P^{s,E_m}(t) = \mathrm{d}t_{r(0)} - \mathrm{d}\tilde{t}^{s(0),E_m} + b_{r,P,\mathrm{ISCB}}^{s,E_m}(t) - \tilde{l}_P^{s,E_m}(t) \end{cases} \quad (6)$$

where the OMC is

$$\tilde{l}_P^s(t) = l_P^s(t) - \Delta \mathrm{d}t_{r(t)} + \Delta \mathrm{d}t^{s(t)} - \sum_{ii=1}^{t-1} \Delta \mathrm{d}t_{r(ii)} + \sum_{ii=1}^{t-1} \Delta \mathrm{d}t^{s(ii)} - M_r^s \cdot \mathrm{zwd}(t) \tag{7}$$

The initial clock offsets of the receiver and satellite, $\mathrm{d}t_{r(0)}$ and $\mathrm{d}\tilde{t}^{s(0)}$, can be obtained by combining (4) and (6). The basic idea of the mixed-differenced model is to use epoch-differenced observations of carrier phase to estimate the variations in the receiver clock, satellite clock and tropospheric delay parameters and then substitute those variations into (6) to update the OMC to obtain a more stable initial clock offset value. The estimated parameters of the mixed-differenced model include the following:

$$\begin{aligned} \mathbf{X}_1 &= \begin{bmatrix} \boldsymbol{\Delta}\mathbf{dt^s} & \boldsymbol{\Delta}\mathbf{dt_r} & \boldsymbol{\Delta}\mathbf{zwd} \end{bmatrix}^T \\ \mathbf{X}_2 &= \begin{bmatrix} \mathbf{dt^{s(0)}} & \mathbf{dt_{r(0)}} & \mathbf{zwd} & \mathbf{b_{ISCB}} \end{bmatrix}^T \end{aligned} \tag{8}$$

In accordance with (4) and (6), the epoch-differenced carrier phase observations and undifferenced pseudorange observations are added into the observation equations in station order. The observation equation of the mixed-differenced model for real-time clock offset estimation can be expressed as follows:

$$\begin{bmatrix} \mathbf{z}_1 \\ \mathbf{z}_2 \\ 0 \end{bmatrix} = \begin{bmatrix} \left[\mathbf{1}_{n_T \times 1}\right] \otimes \mathbf{I}_{n_S \times n_S} & \mathbf{I}_{n_T \times n_T} \otimes \mathbf{A}_{Ti,\Delta\Phi} & \mathbf{0} & \mathbf{0} \\ \mathbf{0} & \mathbf{0} & \left[\mathbf{1}_{n_T \times 1}\right] \otimes \mathbf{I}_{n_S \times n_S} & \mathbf{I}_{n_T \times n_T} \otimes \mathbf{A}_{Ti,P} \end{bmatrix} \cdot \begin{bmatrix} \mathbf{X}_1 \\ \mathbf{X}_2 \\ 0 \end{bmatrix} + \begin{bmatrix} \mathbf{v}_1 \\ \mathbf{v}_2 \\ 0 \end{bmatrix} \tag{9}$$

where

$$\mathbf{A}_{Ti,\Delta\Phi} = \begin{bmatrix} \left[\mathbf{1}_{n_S \times 1}\right] & \mathbf{M}_{n_S \times 1} \end{bmatrix} \tag{10}$$

$$\mathbf{A}_{Ti,P} = \begin{bmatrix} \begin{bmatrix} \mathbf{1}_{n_S \times 1} \end{bmatrix} & \begin{bmatrix} \mathbf{M}_{n_S \times 1} \end{bmatrix} & \begin{bmatrix} \mathbf{I}_{n_G \times n_G} & & & & \\ & \mathbf{I}_{n_R \times n_R} & & & \\ & & \mathbf{I}_{n_C \times n_C} & & \\ & & & \mathbf{I}_{n_E \times n_E} & \\ & & & & \begin{bmatrix} \mathbf{1}_{1 \times n_S} \end{bmatrix} \end{bmatrix} \\ 0 & 0 & \end{bmatrix} \tag{11}$$

here $\otimes$ denotes the Kronecker product (Rao 1973). $\mathbf{1}$ is vector with all elements 1 and $\mathbf{I}$ is identity matrix. $\left[\mathbf{1}_{n_T \times 1}\right] \otimes \mathbf{I}_{n_S \times n_S}$ is the coefficient matrix of the satellite clock parameters of all stations. $\mathbf{A}_{Ti,\Delta\Phi}$ is the epoch-differenced carrier phase observation coefficient matrix, which is unrelated to the satellite clock parameters of the Tith station. $\mathbf{A}_{Ti,P}$ is the undifferenced pseudorange observation coefficient matrix,

which is also unrelated to the satellite clock parameters of the Tith station. $\mathbf{M}_{n_S \times 1}$ is the projection coefficient matrix of the tropospheric parameters.

From the coefficient matrix $\mathbf{A}_{Ti,P}$, it can be found that, unlike the undifferenced model, the mixed-differenced model considering ISCBs synchronizes GPS, GLONASS, BeiDou and Galileo observations to the same datum by adding the estimated parameter ISCBs and applying a zero constraint to the sum of all ISCBs at one station.

There are $n_T \times n_S$ ISCB parameters in (8). According to the assumption stated above (60 stations tracking 110 satellites), the number of ISCB parameters is 6600, too many to permit efficient real-time calculation.

The ISCB parameters do not change over time and are state parameters that are unrelated to other parameters. The receiver-dependent ISCB of each manufacturer remains stable over a long time; the stability for GPS and Galileo is at the centimeter level. For GLONASS is at the decimeter level (Shi et al. 2013; Hauschild and Mon-

tenbruck 2016; Chen et al. 2018a). We achieve the time synchronization of GPS, GLONASS, BeiDou and Galileo by using a single epoch's datum to determine one station's ISCBs. The receivers in the network are unified by selecting one time reference datum, such as one satellite or one

Multi–GNSS RT–Clock Tracking Station
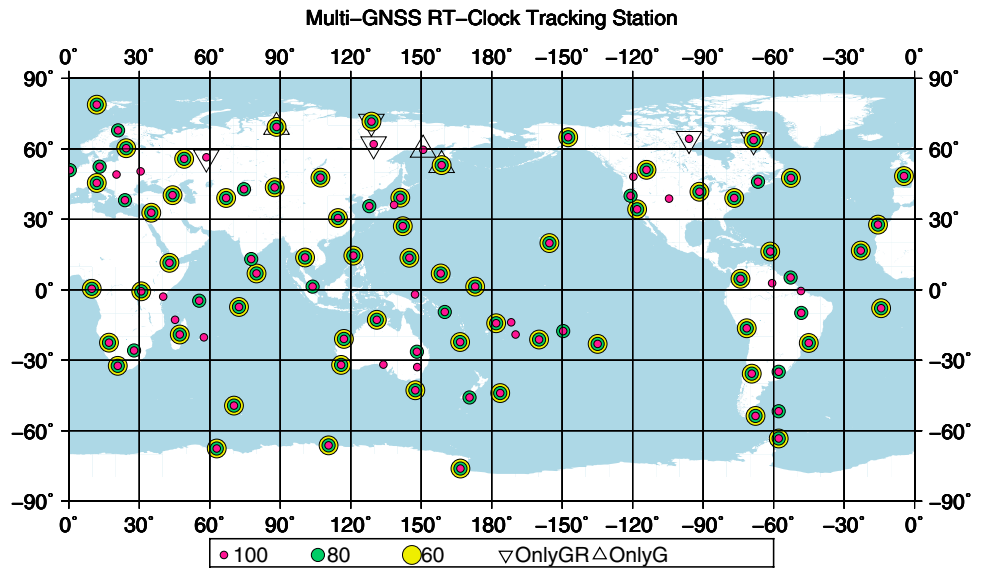
station. As external products similar to precise orbit and station coordinates, the estimated ISCBs of all stations are designed to be introduced into (6) in order to eliminate the bias parameters $\mathbf{b}_{\mathrm{ISCB}}$. This approach greatly reduces the number of parameters to be estimated and further improves the efficiency of multi-GNSS real-time clock offset estimation; then, the mixed-differenced model considering ISCBs can be further simplified as follows:

$$
\begin{cases}
v_P^s(t) = dt_{r(0)} - d\tilde{t}^{s(0)} - \widehat{l}_P^{\,s}(t) \\
v_{\Delta\Phi}^s(t) = \Delta dt_{r(t)} - \Delta dt^{s(t)} + M_r^s \cdot \Delta\mathrm{zwd}(t) - l_{\Delta\Phi}^s(t)
\end{cases}
\tag{12}
$$

where the OMC is updated as follows:

$$
\widehat{l}_P^{\,s}(t) = \tilde{l}_P^s(t) - b_{r,P,\mathrm{ISCB}}^s(t) = l_P^s(t) - \sum_{ii=1}^{t} \Delta dt_{r(ii)} + \sum_{ii=1}^{t} \Delta dt^{s(ii)} - M_r^s \cdot \mathrm{zwd}(t) - b_{r,P,\mathrm{ISCB}}^s(t)
\tag{13}
$$

The undifferenced pseudorange coefficient matrix $\mathbf{A}_{Ti,P}$ is simplified as follows:

$$
\mathbf{A}_{Ti,P} = \left[\, \left[\mathbf{1}_{n_S \times 1} \right] \, \left[\mathbf{M}_{n_S \times 1} \right] \, \right]
\tag{14}
$$

The parameters to be estimated are as follows:

$$
\begin{aligned}
\mathbf{X}_1 &= \left[\, \Delta\mathbf{dt^s} \ \ \Delta\mathbf{dt_r} \ \ \Delta\mathbf{zwd} \, \right]^T \\
\mathbf{X}_2 &= \left[\, \mathbf{dt^{s(0)}} \ \ \mathbf{dt_{r(0)}} \ \ \mathbf{zwd} \, \right]^T
\end{aligned}
\tag{15}
$$

The estimated parameters include only the initial clock, clock difference and tropospheric delay parameters.

Acquisition of multi-GNSS ISCBs with the same datum

As introduced above, a mixed-differenced model considering ISCBs requires the external input of one station's ISCBs with the same datum. B_P^s, satellite-dependent code bias, has been included in the satellite clock products provided by the IGS based on ionospheric-free combined observations (Schaer et al. 1998), i.e., $d\tilde{t}^s = dt0^s + dt^s + B_P^s$, and will be introduced into the carrier phase observations. In addition, the clock offset biases $dt0^s$ will not be completely absorbed by the receiver clock offset. The linearized undifferenced observation equation (1) of the single-station multi-GNSS real-time ISCB estimation model with the same datum is as follows:

$$
\begin{aligned}
v_P^s &= \mathbf{u}^s \cdot \mathbf{dx} + dt_r + \left(b_{r,P,\mathrm{ISCB}}^s - dt0^s \right) + M_r^s \cdot \mathrm{zwd} - l_P^s \\
v_\Phi^s &= \mathbf{u}^s \cdot \mathbf{dx} + dt_r + \left(b_{r,P,\mathrm{ISCB}}^s - dt0^s \right) + \widehat{N}_r^{\,s} + M_r^s \cdot \mathrm{zwd} - l_\Phi^s
\end{aligned}
\tag{16}
$$

where $\widehat{N}_r^{\,s} = N_r^s + \left(b_\Phi^s - b_{r,P,\mathrm{ISCB}}^s \right) - \left(B_\Phi^s - B_P^s \right)$. The ISCB and IFB parameters are added to the linearized equations for every epoch as follows:

Table 2 Multi-GNSS real clock offset estimation strategy considering ISCBs

Parameter	Model
Observations	
Observations	Undifferenced pseudorange/carrier phase; epoch-differenced carrier phase
Satellites	Approximately 110 GPS/GLONASS/BeiDou/Galileo satellites
Prior information	P1: 1.0 m; L1: 0.02 cycles
Cut-off elevation	7°
Observation weights	$p = 1$, elev $> 30°$
	$p = 2\sin(\text{elev})$, elev $\leq 30°$
Intervals	Real-time 1 s/post-test 30 s
Reference frame	
Time system	GPS time
Inertial reference frame	ICRF J2000.0
ECEF	ITRF2014 (Altamimi et al. 2016)
Precession and nutation	IAU2000
EOP	IERS C04 (Bizouard and Gambis 2009)
Solar and lunar ephemerides	JPL DE405
Error correction	
Ocean tides	IERS conventions 2003
Earth solid tides	IERS conventions 2003
Phase wind-up	Correction (Wu et al.1993)
Phase center offset (PCO)/phase center variation (PCV)	
Satellite	
GPS, Galileo PCO: IGS14.atx (Rebischung and Schmid 2016);	
BeiDou-2 GEO PCO: IGS M-GEX;	
BeiDou-2 IGSO/MEO PCO: ESA Mode (Dilssner et al. 2014);	
BeiDou-3 MEO: www.beidou.gov.cn	
GPS PCV: IGS14.atx; BeiDou, Galileo PCV: uncorrected	
Receiver	
GPS PCO: IGS14.atx; BeiDou, Galileo PCO: same as GPS;	
GPS PCV: IGS14.atx; BeiDou, Galileo PCV: same as GPS	
Relativistic effects	Correction
Parameters	
Adjustment method	Square-root information filtering (Bierman 1977)
Reference clock	One satellite clock
Orbit	Fixed
Station coordinates	Fixed
Tropospheric delay	Saastamoinen model + GMF mapping function random-walk process for each epoch
Satellite/receiver clock	Estimated as white noise
Initial clock	Estimated as constant parameters
Ambiguity	Estimated using the undifferenced model, eliminated with epoch-differenced phase/estimated if exit cycle slips
ISCBs	Estimated in the undifferenced model with zero-mean condition, Eliminated with epoch-differenced phase/corrected in the mixed-differenced model

Fig. 2 ISCBs for GPS, GLO-
NASS, BeiDou-2/3 and Galileo
satellites for all 100 stations
with the same datum
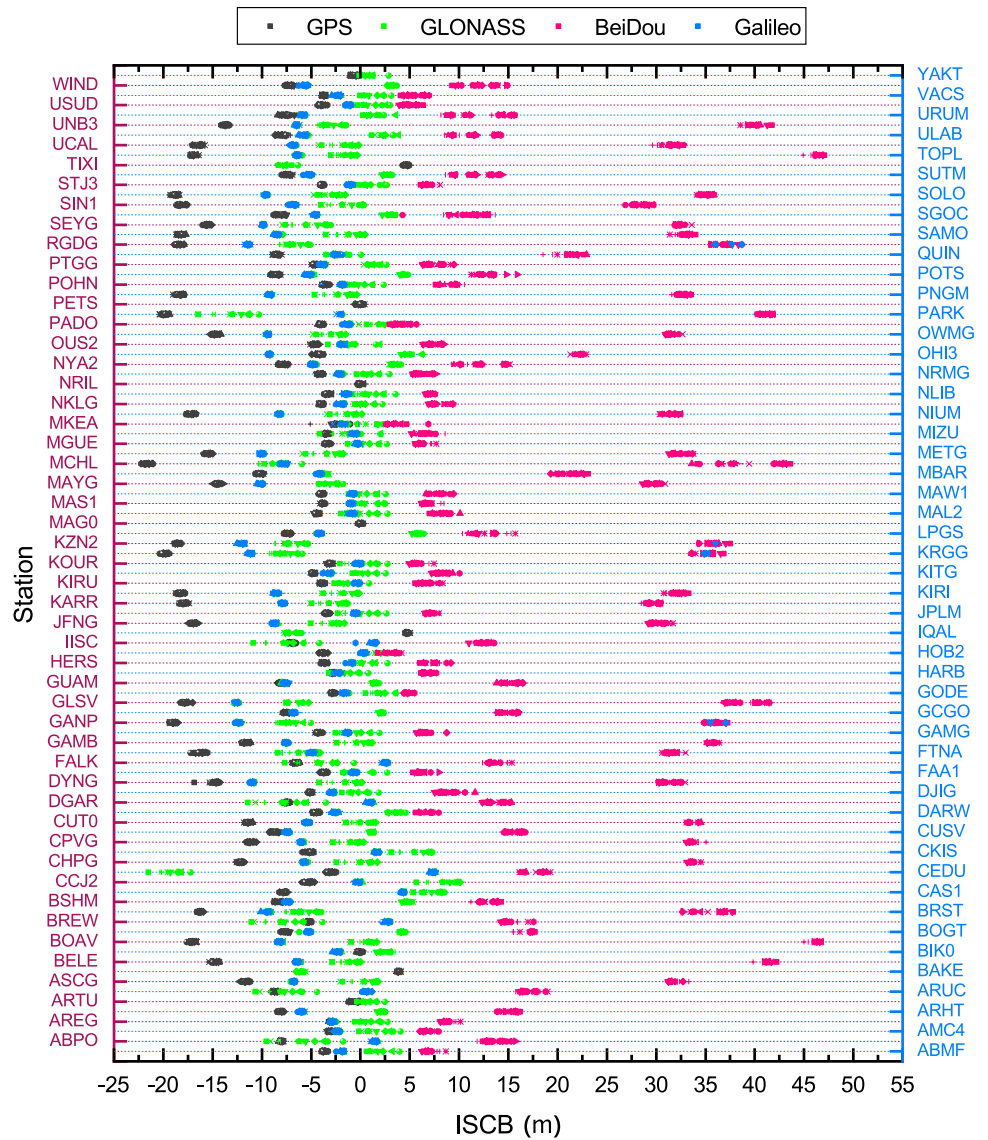
The ISCB parameters are estimated as constant, and a
zero constraint is applied to the sum of all ISCBs at one
station to separate the ISCBs from every epoch. Then, the
multi-GNSS ISCBs with the same datum can be obtained
as follows:

$$
\begin{cases}
\text{ISCB}^{G_i} = b^{s,G_i}_{r,P,\text{ISCB}} - \mathrm{d}t0^{s,G_i} \\
\text{IFB}^{R_j} = b^{s,R_j}_{r,P,\text{ISCB}} - \mathrm{d}t0^{s,R_j} \\
\text{ISCB}^{C_k} = b^{s,C_k}_{r,P,\text{ISCB}} - \mathrm{d}t0^{s,C_k}_k \\
\text{ISCB}^{E_m} = b^{s,E_m}_{r,P,\text{ISCB}} - \mathrm{d}t0^{s,E_m}
\end{cases}
\tag{17}
$$

$$
\sum_{i=1}^{n_G} \text{ISCB}^{G_i} + \sum_{j=1}^{n_R} \text{IFB}^{R_j} + \sum_{k=1}^{n_C} \text{ISCB}^{C_k} + \sum_{m=1}^{n_E} \text{ISCB}^{E_m} = 0
\tag{18}
$$

In the multi-GNSS single-station real-time ISCB esti-
mation model, the estimated ISCB includes the receiver-
dependent ISCB and the clock offset biases in the clock
products.

Performance analysis

Three multi-GNSS global networks with 60, 80 and 100
stations are defined based on the multi-GNSS experiment
(M-GEX) of the IGS (http://mgex.igs.org), as shown in
Fig. 1. Data from days of the year (DOYs) 359 to 365 in
2019 are selected. The multi-GNSS precise orbit products
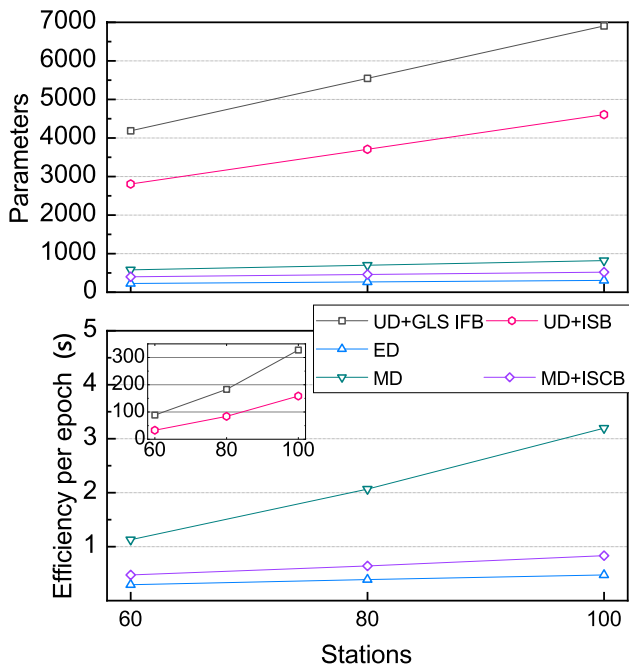
Fig. 3 Comparison of the numbers of parameters and single-epoch estimation efficiencies for various multi-GNSS clock estimation models

provided by the GFZ German Research Centre for Geosciences are selected (Montenbruck et al. 2017), in which the BeiDou-2 + 3 precise orbits are based on B1I + B3I signals. The multi-GNSS real clock offset estimation strategy is summarized in Table 2.

Multi-GNSS ISCBs with the same datum

Figure 2 shows the distribution of the ISCBs for GPS, GLONASS, BeiDou-2/3 and Galileo (GRCE) for all 100 stations as estimated with the additional constraint (18). There are obvious clustering phenomena of the GRCE ISCBs for individual stations, and the overall differences between the GRCE ISCBs are also the ISB parameters estimated in (3) using the undifferenced model.

It can be seen from this figure that compared to the higher aggregation of the GPS and Galileo satellites, the ISCB consistency of some GLONASS and BeiDou satellites is poor. When the ISCB is assumed to be a common parameter to be estimated in the undifferenced model, this will cause the receiver-dependent differences of the ISCBs to be ignored. These ISCB differences will then be brought into the real-time precise clock offset products
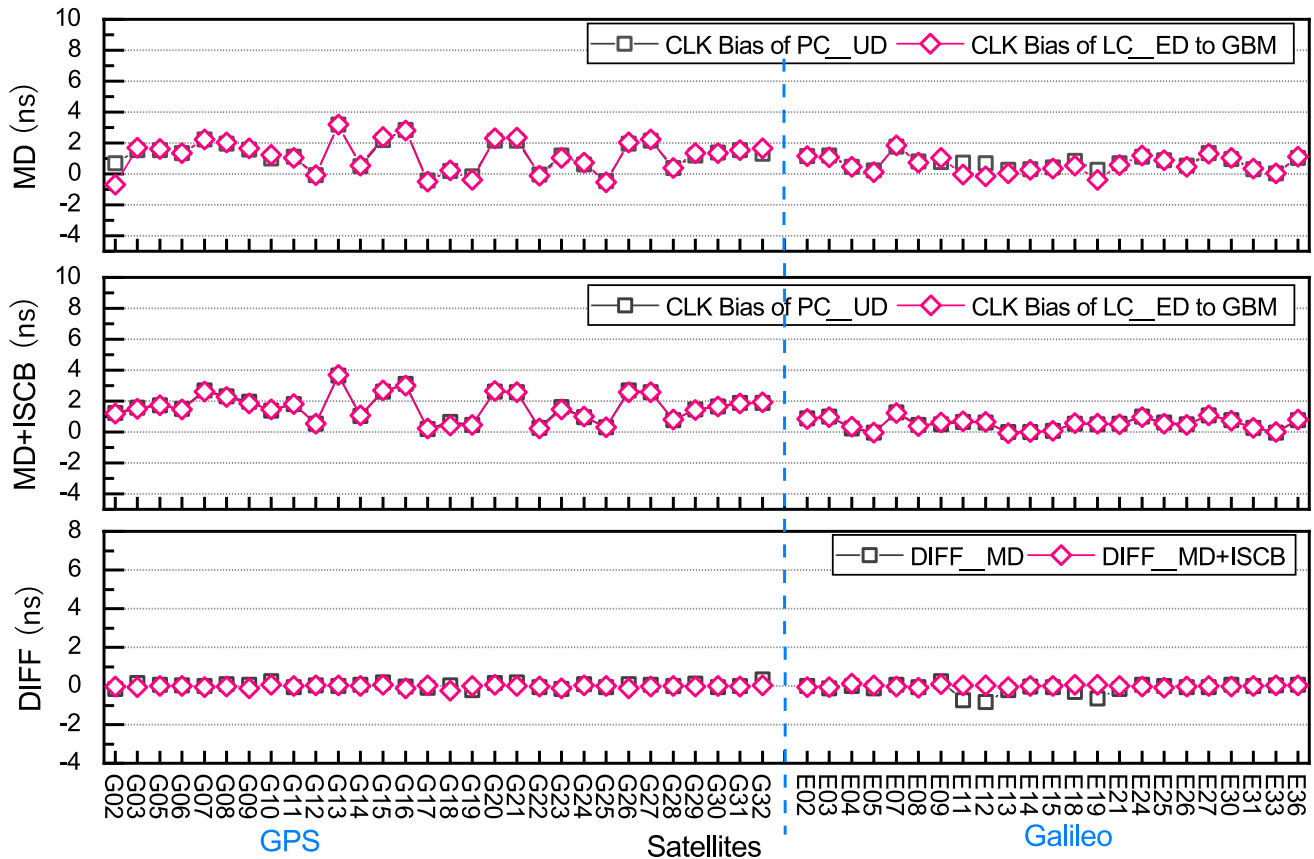
Fig. 4 Consistencies between the clock biases of PC_UD and LC_ED for GPS and Galileo before and after ISCB correction
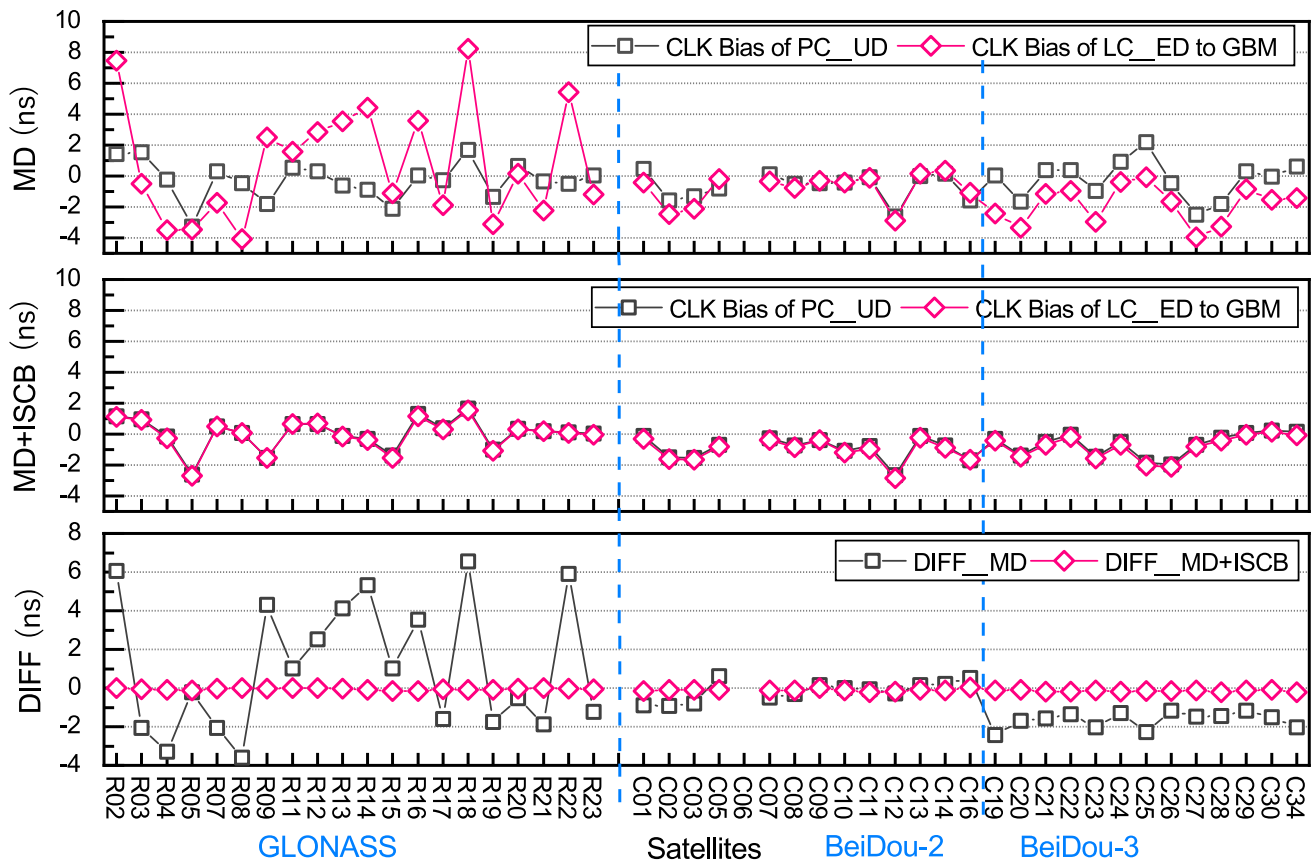
Fig. 5 Consistencies between the clock biases of PC_UD and LC_ED for GLONASS and BeiDou before and after ISCB correction

and create unequal clock offset biases (Hauschild et al. 2019).

Parameters and efficiency

For the 110 estimated satellite clocks of GRCE, Fig. 3 shows a comparison of the numbers of parameters and estimation efficiencies for different models in the three cases of global networks consisting of 60, 80 and 100 stations. UD + GLS IFB represents undifferenced model estimating the GLONASS IFBs; UD + ISB represents the undifferenced model estimating only the ISBs; ED represents the epoch-differenced model; MD represents mixed-differenced model; MD + ISCB represents mixed-differenced model considering ISCBs.

As seen from this figure, the undifferenced models cannot meet the 5 s updating requirement for real-time clock offsets recommended by the IGS due to the large number of parameters to be estimated. As the number of stations increases, the estimation efficiency of the MD model also

gradually degrades to several seconds. Based on the MD model, the multi-GNSS real-time clock offset estimation model considering ISCBs, designed as (MD + ISCB), eliminates a large number of systematic bias parameters, with a parameter elimination rate of 95%, thereby improving the single-epoch estimation efficiency to meet the requirements for a 1 Hz update frequency. With the selection of appropriate hardware environments and global stations, this model can fully meet the incremental development needs of real-time clock estimation for multi-GNSS, such as BeiDou-3, Galileo and other regional navigation systems.

Initial satellite clock bias

The core of a mixed-differenced model consists of estimating the initial clock offset bias based on undifferenced pseudorange observations and the estimation of clock offset differences between consecutive epochs based on epoch-differenced carrier phase observations. The initial clock offset bias obtained from the undifferenced pseudorange

Fig. 6 Time sequences of initial clock offset biases before and after ISCB correction
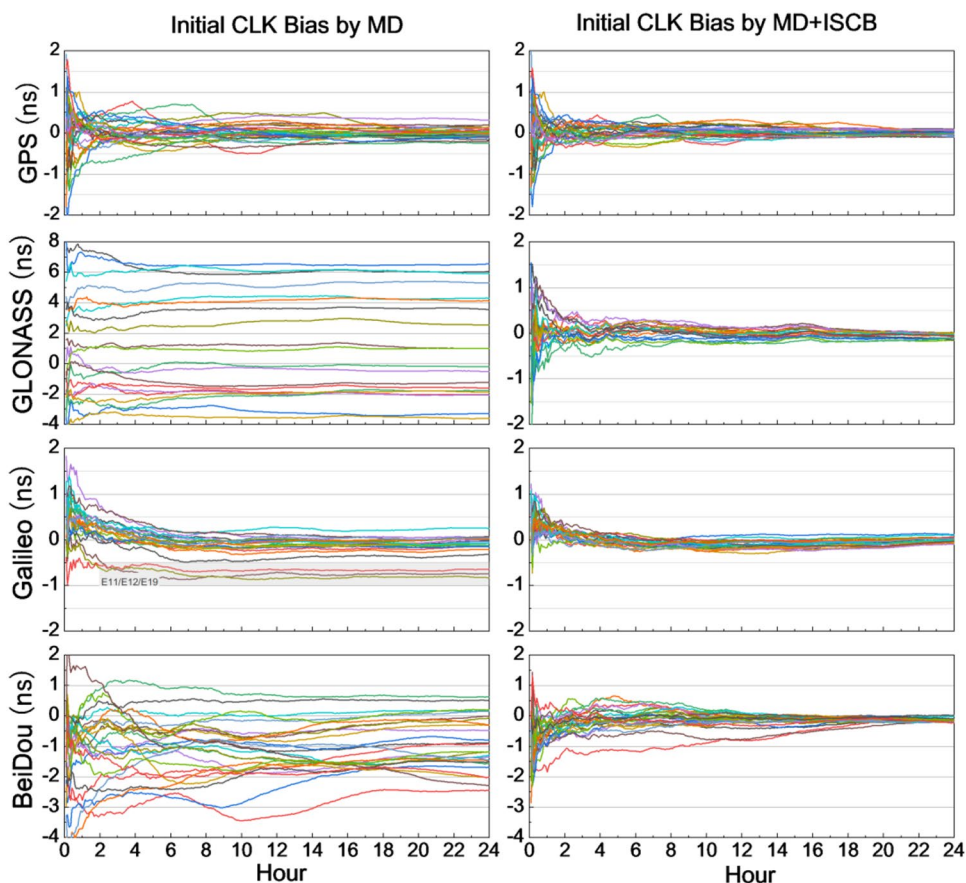
observations should theoretically be a constant, which determines the precise zero-value bias characteristic of the clock offsets, namely, whether there is systematic bias relative to the reference precise clock products.

To analyze the influence of ISCB correction on the initial clock offset bias in the mixed-differenced models, GFZ multi-GNSS clock products (GBM) are selected as the reference clock products. We analyze the initial clock offset obtained from undifferenced pseudorange (clock bias of PC_UD) and relative clock offset from epoch-differenced carrier phase (clock bias of LC_ED) separately. According to the mixed-differenced model theory, the clock bias of PC_UD should be consistent with the clock bias of LC_ED. These factors affect each other to form the absolute clock.

Figures 4 and 5 show the consistency between the clock biases of PC_UD and LC_ED before and after ISCB correction, respectively. Figure 5 shows that there is high consistency between the two biases of GLONASS and BeiDou obtained using the MD + ISCB model, with the differences being near zero. The MD + ISCB model resolves the clustering phenomenon between BeiDou-2 and BeiDou-3 in the MD model and yields an absolute clock offset with zero bias relative to the reference precise clock products.

By subtracting the clock bias of LC_ED, the initial clock offset bias can be obtained. Figure 6 shows time

sequences of the initial clock offset biases before and after ISCB correction. Because the initial clock offset is estimated to be constant, convergence behavior is observed with an increasing number of observations. As seen from the figure, the initial clock offsets of GLONASS and BeiDou estimated using the MD model have unequal biases, and there are clustered biases between the three Galileo In-Orbit Validation (IOV) satellites (E11, E12, and E19) and the other Full Operational Capability (FOC) satellites. For the initial clock offset biases considering ISCBs, convergence is achieved in approximately 1 h, which is a significant improvement compared to the MD model without ISCB correction, and after convergence, the biases remain stable and close to zero.

As seen, the initial clock offset bias can remain stable after a sufficient period of estimation. Therefore, this parameter in the MD model can be removed from among the parameters to be estimated after convergence, resulting in improved efficiency.

Real-time clock performance

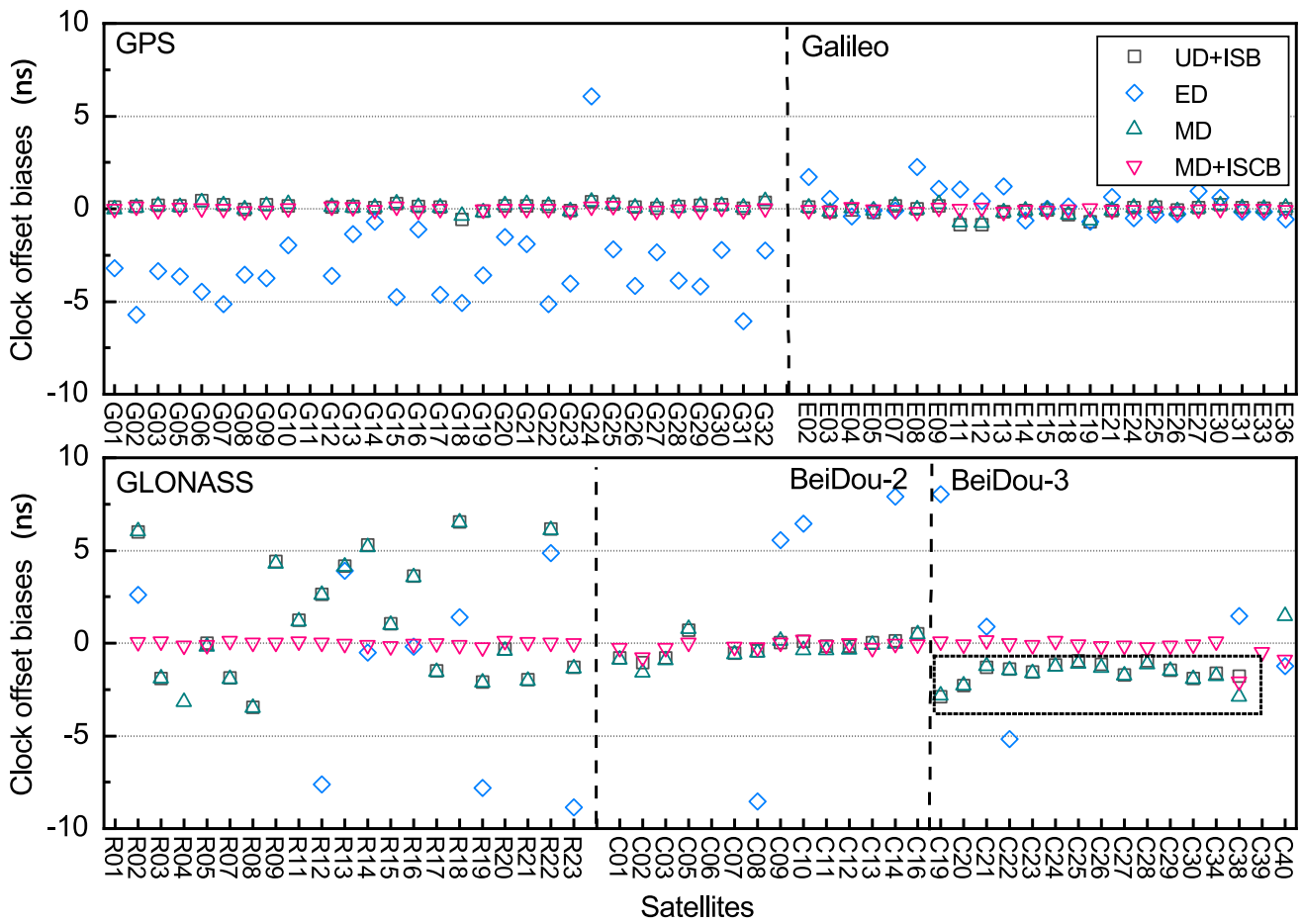We use (19) to analyze the performance of the real-time clock offset estimation model.

Fig. 7 Clock offset biases obtained using UD + ISB, ED, MD and MD + ISCB

Table 3 Clock offset biases, RMS, and STD values of the clock offsets obtained using UD + ISB, ED, MD and MD + ISCB (ns)

Type	UD + ISB	ED	MD	MD + ISCB	MD + ISCB Improvement compared to MD
Clock offset biases					
GPS	0.15	− 3.05	0.13	0.00	–
GLONASS	1.41	− 19.57	1.12	0.00	–
Galileo	− 0.12	0.29	− 0.10	− 0.04	–
BeiDou	− 0.87	17.78	− 0.98	− 0.13	–
RMS					
GPS	0.22	3.47	0.21	0.13	40%
GLONASS	2.93	20.91	2.95	0.12	96%
Galileo	0.27	0.66	0.26	0.17	37%
BeiDou	1.08	26.92	1.16	0.25	78%
STD					
GPS	0.15	0.08	0.15	0.10	33%
GLONASS	0.16	0.04	0.16	0.09	46%
Galileo	0.15	0.14	0.15	0.15	2%
BeiDou	0.32	0.18	0.31	0.17	45%
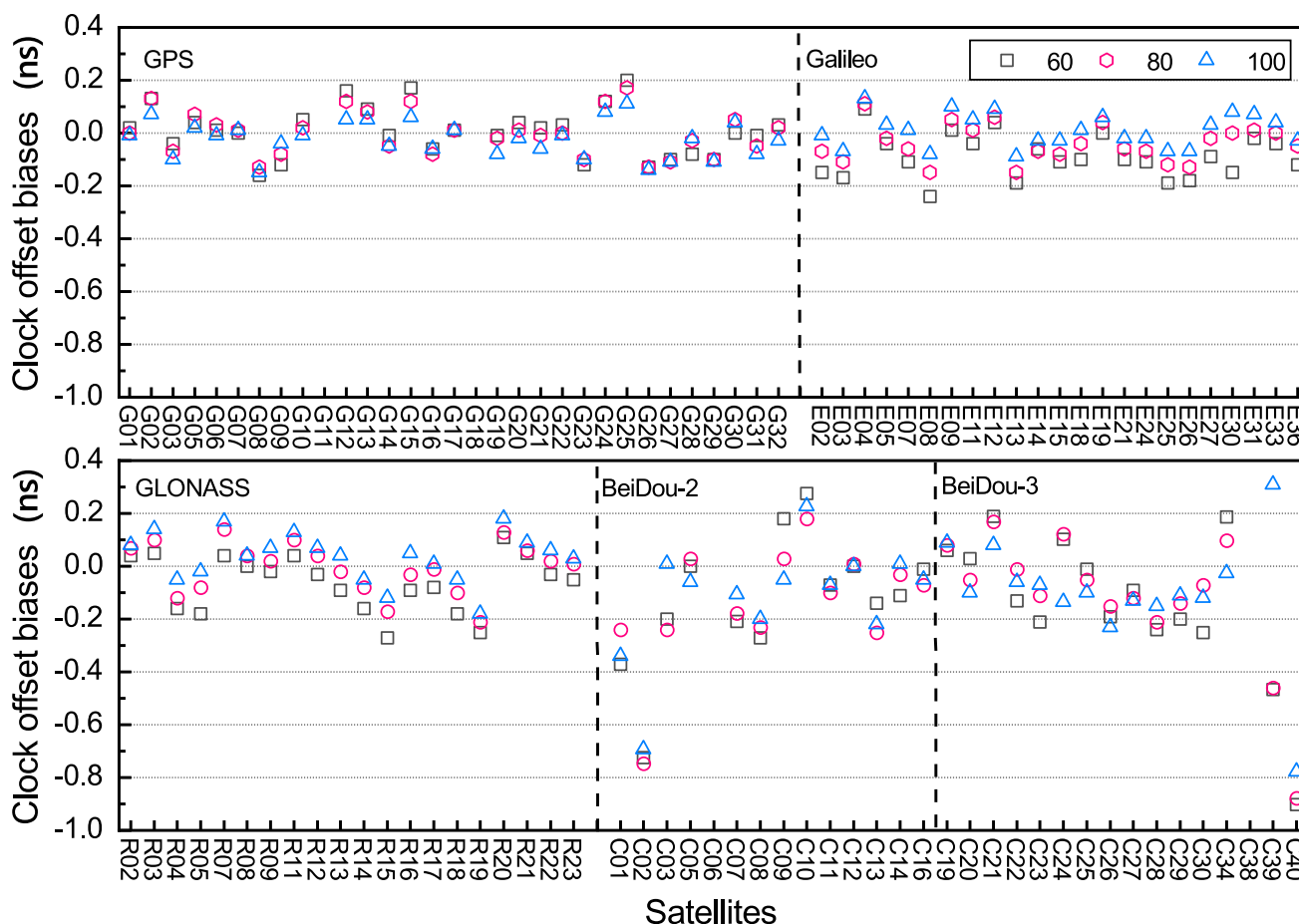
Fig. 8 Clock offset biases obtained using MD + ISCB for 60, 80 and 100 stations

$$\mathrm{STD} = \sqrt{\frac{\sum_{i=1}^{n}\left(\Delta_i - \overline{\Delta}\right)^2}{n - 1}}$$

$$\mathrm{RMS} = \sqrt{\frac{\sum_{i=1}^{n}\left(\Delta_i\right)^2}{n}} \tag{19}$$

where Δ_i is the quadratic clock difference from the reference clock products after the subtraction of the time datum in the ith epoch. $\overline{\Delta}$, the average of these quadratic clock differences, can be used to evaluate the clock offset biases characteristics of these models; the STD reflects the stability, and the RMS reflects the absolute accuracy.

Taking the test results for 80 global stations over one week as an example, Fig. 7 shows the clock offset biases obtained using the UD + ISB, ED, MD and MD + ISCB models (G06, R01, E01, and C06, respectively, are selected as the reference satellites to eliminate systematic bias). We

find that for the ED model, there are nanosecond-level unequal biases compared to the reference precise clock products. Based on the analysis above, these biases are caused by the introduction of an outside initial clock offset. Even though the GPS and Galileo clock offsets estimated using the undifferenced and mixed-differenced models are absolute clocks, there are obvious biases for the GLONASS and BeiDou clock solutions. When C06 is selected as the reference satellite to eliminate systematic bias, there is a clustering phenomenon between BeiDou-2 and BeiDou-3 in the undifferenced and mixed-differenced models, as shown in the rectangle in the bottom panel of Fig. 7.
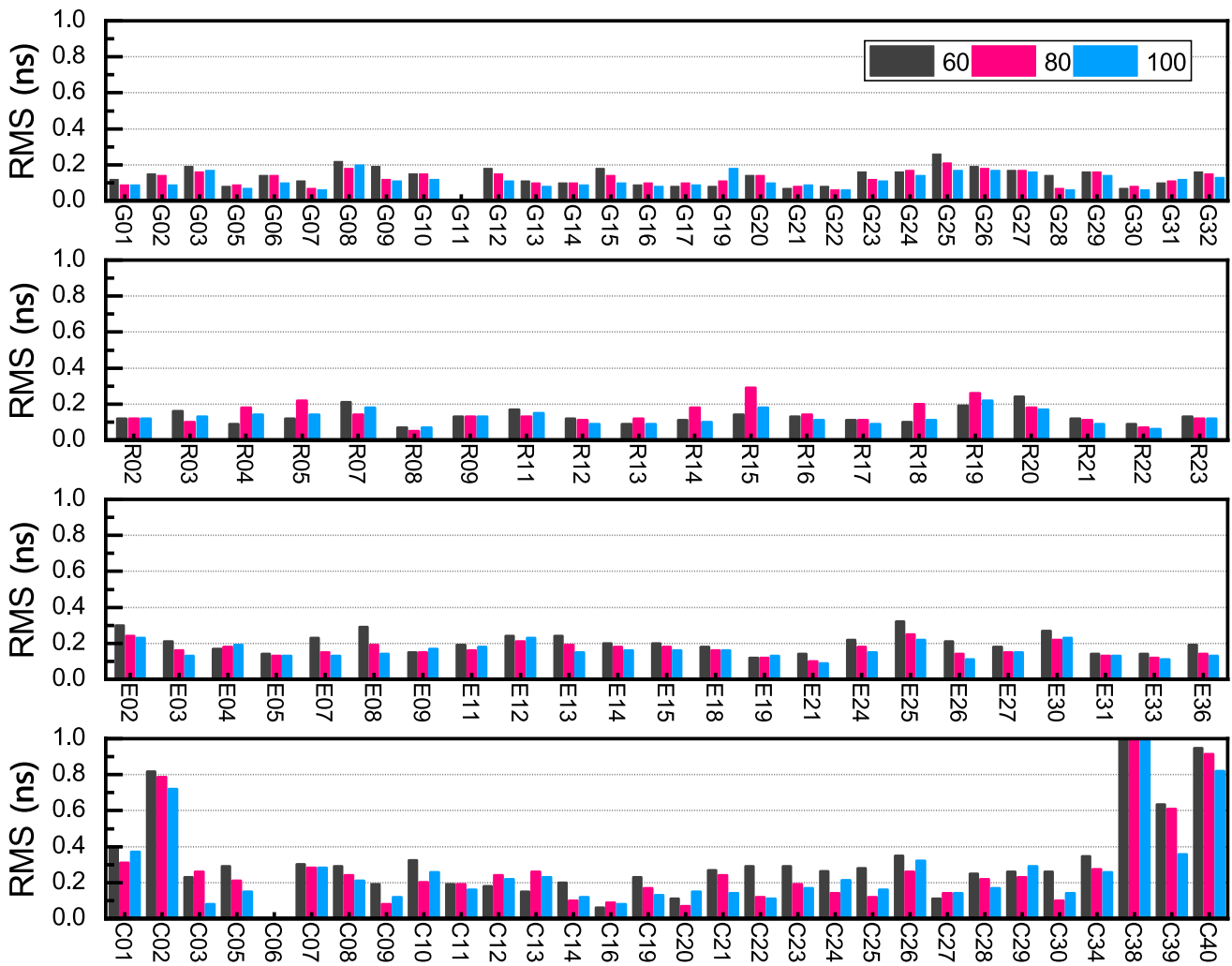
Fig. 9 RMS values of the clock offset differences obtained using MD + ISCB for 60, 80 and 100 stations

Table 3 lists the real-time clock offset biases, RMS and STD values for GPS, GLONASS, Galileo and BeiDou as obtained using the UD + ISB, ED, MD and MD + ISCB models. We find that the MD + ISCB model can obtain a precise absolute clock offset with zero-bias characteristics, which can clearly eliminate the systematic bias problems of the GLONASS and BeiDou clock products. The real-time clock RMS values for GPS, GLONASS, Galileo and BeiDou are 0.13 ns, 0.12 ns, 0.17 ns and 0.25 ns, respectively, being improved by approximately 63% compared to MD model. Corresponding STD values are 0.10 ns, 0.09 ns, 0.15 ns and 0.17 ns, respectively, at the same level as ED model and superior to the undifferenced and MD model. The clock STDs for GLONASS and BeiDou are improved by 45%

compared to those of the MD model. The reason for the lack of improvement in the Galileo STD may be that the Galileo satellites show small variations in the ISCBs, and most of these consistent ISCBs can be absorbed into the solution.

Impact of the number of stations in the network

Figures 8, 9 and 10 and Table 4 present comparisons of the clock offset biases, RMS values and STD values obtained with MD + ISCB for 60, 80 and 100 stations. According to Table 4, the precise absolute clock offset can be obtained by considering only 60 multi-GNSS stations. Especially for BeiDou, as the number of stations increases, the performance will improve.
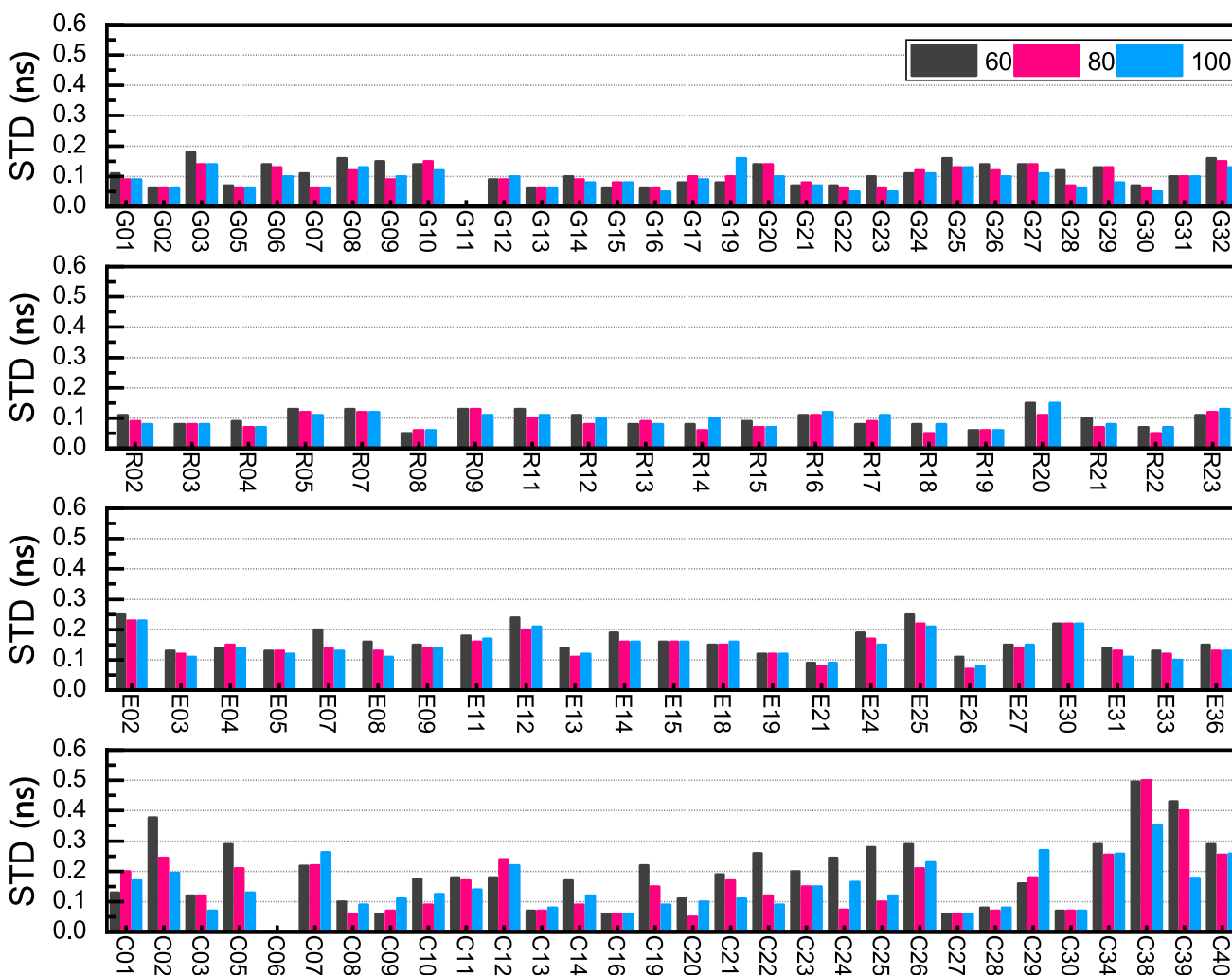
Fig. 10 STD values of the clock offset differences obtained using MD+ISCB for 60, 80 and 100 stations

Conclusion

We introduce the basic theory and main challenges of real-time GNSS clock offset estimation using undifferenced and epoch-differenced models. To address the common clock offset biases problem in real-time precise clock products, an ISCB correction method is introduced, and a multi-GNSS real-time precise clock estimation model considering ISCBs is proposed. This model can produce zero-bias absolute precise real-time clock offsets, thereby resolving the systematic bias problems in the GLONASS and BeiDou clock offsets. The real-time clock RMS values for GPS, GLONASS, Galileo and BeiDou are 0.13 ns, 0.12 ns, 0.17 ns and 0.25 ns, respectively, representing an improvement by approximately 63% compared to mixed-differenced model. Corresponding STDs are 0.10 ns, 0.09 ns, 0.15 ns and 0.17 ns, respectively, at the same level as epoch-differenced model and superior to undifferenced and mixed-differenced models. The clock STDs of GLONASS and BeiDou are improved by 45% compared to those of the mixed-differenced model.

On the basis of the mixed-differenced model, which eliminates ambiguity parameters, the multi-GNSS real-time clock offset estimation model considering ISCBs presented here further eliminates a large number of bias parameters, achieving a parameter elimination rate of 95%, which further improves the single-epoch estimation efficiency and enables an updating rate on the level of seconds. With the selection of appropriate hardware environments and global stations, this model can fully meet the incremental development needs of real-time clock offset estimation for multi-GNSS, such as BeiDou-3, Galileo and other regional navigation systems.

Table 4 Clock offset biases, RMS, and STD values of the clock offsets obtained using MD + ISCB for 60, 80 and 100 stations (ns)

Types	60	80	100
Clock offset biases			
GPS	0.01	0.00	− 0.02
GLONASS	− 0.06	0.00	0.03
Galileo	− 0.09	− 0.04	0.01
BeiDou	− 0.09	− 0.09	− 0.10
RMS			
GPS	0.14	0.13	0.11
GLONASS	0.13	0.12	0.12
Galileo	0.20	0.17	0.16
BeiDou	0.27	0.21	0.21
STD			
GPS	0.11	0.1	0.09
GLONASS	0.10	0.09	0.09
Galileo	0.16	0.15	0.14
BeiDou	0.18	0.13	0.14

References

Altamimi Z, Rebischung P, Métivier L, Collilieux X (2016) ITRF2014: a new release of the International Terrestrial Reference Frame modeling nonlinear station motions. J Geophys Res 121(8):6109–6131

Bierman G (1977) Factorization methods for discrete sequential estimation. Academic Press Inc., New York

Bizouard C, Gambis D (2009) The combined solution C04 for earth orientation parameters consistent with international terrestrial reference frame 2005. In: Geodetic reference frames, IAG symposium134, Munich, Germany, October 9–14, pp 265–270

Bock H, Dach R, Jäggi A, Beutler G (2009) High-rate GPS clock corrections from CODE: Support of 1 Hz applications. J Geodesy 83(11):1083–1094

Chen L, Li M, Hu Z, Fang C, Geng C, Zhao Q, Shi C (2018a) Method for real-time self-calibrating GLONASS code inter-frequency bias and improvements on single point positioning. GPS Solut 22(4):111

Chen L, Zhao Q, Hu Z, Jiang X, Geng C, Ge M, Shi C (2018b) GNSS global real-time augmentation positioning: real-time precise satellite clock estimation, prototype system construction and performance analysis. Adv Space Res 61(1):367–384

Chen Y, Yuan Y, Zhang B, Liu T, Ding W, Ai Q (2018c) A modified mix-differenced approach for estimating multi-GNSS realtime satellite clock offsets. GPS Solut 22(3):72

Dach R, Schaer S, Hugentobler U (2006) Combined multi-system GNSS analysis for time and frequency transfer. In: Proceedings of the 20th European frequency and time forum EFTF06, 2006, Braunschweig, Germany, pp 530–537

Dilssner F, Springer T, Schönemann E, Enderle W (2014) Estimation of satellite antenna phase center corrections for BeiDou. In: IGS workshop 2014, Pasadena, USA, June 23–27

Ge M, Gendt G, Rothacher M, Shi C, Liu J (2008) Resolution of GPS carrier phase ambiguities in precise point positioning (PPP) with daily observations. J Geodesy 82(7):389–399

Ge M, Chen J, Douša J, Gendt G, Wickert J (2012) A computationally efficient approach for estimating high-rate satellite clock corrections in realtime. GPS Solutions 16(1):9–17

Hadas T, Bosy J (2015) IGS RTS precise orbits and clocks verification and quality degradation over time. GPS Solut 19(1):93–105

Hauschild A, Montenbruck O (2016) The effect of correlator and front-end design on GNSS pseudorange biases for geodetic receivers. Navigation 63(4):443–453

Hauschild A, Steigenberger P, Montenbruck O (2019) Inter-receiver GNSS pseudorange biases and their effect on clock and DCB estimation. In: Proceedings of ION GNSS+ 2019, Institute of Navigation, Miami, Florida, USA, September 16–20, pp 3675–3685

He C, Lu X, Guo J, Su C, Wang W, Wang M (2020) Initial analysis for characterizing and mitigating the pseudorange biases of BeiDou navigation satellite system. Satellite Navigation 1(1):3

Montenbruck O et al (2017) The multi-GNSS experiment (MGEX) of the international GNSS service (IGS)-achievements, prospects and challenges. Adv Space Res 59(7):1671–1697

Rao C (1973) Linear statistical influence and its applications. Wiley, New York

Rebischung P, Schmid R (2016) IGS14/igs14.atx: a new framework for the IGS products. In: American geophysical union fall meeting 2016, San Francisco, USA, December 12–16

Schaer S, Gurtner W, Feltens J (1998) IONEX: The ionosphere map exchange format version 1. In: Proceedings of the IGS AC workshop, Darmstadt, Germany, February 9–11

Shi C, Yi W, Song W, Lou Y, Yao Y, Zhang R (2013) GLONASS pseudorange inter-channel biases and their effects on combined GPS/GLONASS precise point positioning. GPS Solut 17(4):439–451

Song W, Yi W, Lou Y, Shi C, Yao Y, Liu Y, Mao Y, Xiang Y (2014) Impact of GLONASS pseudorange inter-channel biases on satellite clock corrections. GPS Solut 18(3):323–333

Wu J, Wu S, Hajj G, Bertiger W, Lichten S (1993) Effects of antenna orientation on GPS carrier phase. Manuscr Geod 18(2):91–98

Wübbena G, Schmitz M, Bagge A (2005) PPP-RTK: precise point positioning using state-space representation in RTK networks. In: ION GNSS 2005, Institute of Navigation, Long Beach, California, USA, September 13–16, pp 2584–2594

Zhang W, Lou Y, Gu S, Shi C, Haase J, Liu J (2016) Joint estimation of GPS/BDS real-time clocks and initial results. GPS Solutions 20(4):665–676

Zhang X, Li X, Guo F (2011) Satellite clock estimation at 1 Hz for real-time kinematic PPP applications. GPS Solutions 15(4):315–324

Publisher's Note   Springer Nature remains neutral with regard to jurisdictional claims in published maps and institutional affiliations.

Liang Chen received his master's degree in 2012 and a doctorate in 2020 from Wuhan University, where he is now a senior engineer and a Postdoc of Beihang University. He visited the German Research Centre for Geosciences (GFZ) as an academic scholar in 2016. His current research focuses primarily on multi-GNSS PPP, real-time precise clock estimation, precise orbit determination and GNSS wide-area augmentation.

Fu Zheng is currently an assistant research fellow at the research institute for frontier science, Beihang University. He received his Ph. D. in Geodesy and Surveying Engineering from Wuhan University in 2017. His current research mainly focuses on multi-frequency GNSS PPP and real-time GNSS applications.
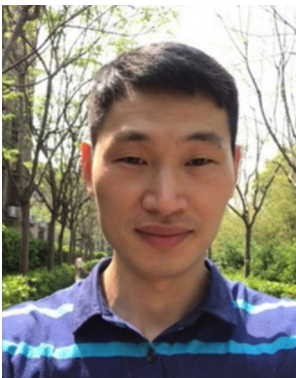
Min Li received his master's degree and a doctorate from Wuhan University in 2007 and 2011, respectively, where is a professor at the GNSS Research Center. His current research lies in precise orbit determination for GNSS.

Chuang Shi is currently a professor at the research institute for frontier science, Beihang University. He graduated from Wuhan Institute of Surveying and Mapping (current Wuhan University) and obtained his Ph. D. in 1998. His research interests include network adjustment, precise orbit determination for GNSS satellites and LEOs, as well as real-time PPP.

Ying Zhao is an engineer at the National Quality Inspection and Testing Center for Surveying and Mapping Products. She received a master's degree from the Chinese Academy of Surveying and mapping in 2013. His current research mainly focuses on GNSS applications on geography status investigation.

Zhigang Hu is an associate professor at the GNSS Research Center at Wuhan University in China. He received his master's degree and a doctorate from Wuhan University in 2008 and 2013, respectively. His current research lies in precise orbit determination for GNSS as well as the performance evaluation for the BeiDou satellite navigation system.